Assessing the impact of valence *sd* neutrons and protons on fusion

Varinderjit Singh, J. Vadas, T.K. Steinbach, B. B. Wiggins, S. Hudan, R. T. deSouza[1,*]

Department of Chemistry and Center for Exploration of Energy and Matter, Indiana University
2401 Milo B. Sampson Lane, Bloomington, IN 47408, USA

arXiv:2010.05720v2 [nucl-ex] 3 Mar 2021

Abstract

Experimental near-barrier fusion cross-sections for ^{17}F + ^{12}C are compared to the fusion excitation functions for ^{16,18}O, ^{19}F, and ^{20}Ne ions on a carbon target. Comparison of the reduced fusion cross-section for the different systems accounts for the differing static size of the incident ions and changes in fusion barrier. Remaining trends of the fusion cross-section above the barrier are observed. These trends are interpreted as the interplay of the *sd* protons and neutrons. The experimental data are also compared to a widely-used analytic model of near-barrier fusion, a time-dependent Hartree-Fock model, and coupled channels calculations.

Keywords: near-barrier fusion, RIB fusion, fusion enhancement

1. Introduction

Nuclear fusion is a topic of considerable interest both from a fundamental perspective as well as in the field of nuclear astrophysics [1]. Nuclei just beyond a closed shell present a unique opportunity to probe the interplay of shell and collective effects on the fusion process. In particular, light nuclei just beyond the $1p_{1/2}$ shell, namely isotopes of oxygen, fluorine, and neon are good candidates for examination. In this work, the fusion of various isotopes of these elements with a carbon target at near-barrier energies is examined. The results of this work, which combines both stable and radioactive beams, points to the potential of low-energy beams at radioactive beam facilities [2, 3] for examining the impact of neutron-excess on fusion.

Addition of neutrons and protons just beyond the $1p_{1/2}$ shells of ^{16}O clearly changes both the matter and charge distributions of the nuclei. Theoretical calculations indicate that for a large neutron excess, e.g. ^{24}O as compared to ^{16}O, fusion with ^{16}O target is significantly enhanced [4]. The impact of adding just a few neutrons or protons beyond the $1p_{\frac{1}{2}}$ shell on fusion is less clear. With increased atomic or mass number, the fusion barrier and consequently the fusion cross-section is clearly impacted. We propose to go beyond these trivial systematic differences and examine the detailed differences in the fusion cross-section. A particularly interesting case to investigate is fusion of the nucleus ^{17}F which exhibits a proton-halo when in its $2s_{1/2}$ excited state [5]. It is presently unclear whether an increased radial extent results in a fusion enhancement or weak binding results in a decreased fusion cross-section. For the case of ^{17}F + ^{208}Pb, neither an enhancement nor a suppression of fusion was observed relative to ^{19}F + ^{208}Pb [7]. However, in the case of fusion with a large target nucleus, such as ^{208}Pb, the impact of adding two neutrons on fusion might be diminished. To examine the impact on fusion of adding a few protons and neutrons to the *sd* shell we measure fusion for ^{17}F + ^{12}C and compare it with fusion induced by O, F, and Ne beams on ^{12}C.

2. Experimental Details

Discovery of halo nuclei, notably ^{11}Li [8, 9] was achieved through systematic examination of the interaction cross-sections for lithium isotopes. At high incident energy one expects the sudden approximation to be valid in describing the collision of the nuclei. Consequently, the nuclear densities do not have enough time to rearrange as the projectile and target nuclei come into contact. Thus a measurement of the interaction cross-section at high energy probes the nuclear size and other geometrical features such as deformation, all of which are considered "static" [8]. Hence, the measured interaction cross-section, σ_I, provides a direct and effective measure of the extent of the matter distribution.

To better understand the change in the static size of the different nuclei considered in this work, we examine the interaction cross-sections measured at high energy. Presented in Table 1 are σ_I for O, F, and Ne nuclei with a carbon target [10] with the number of protons and neutrons in the *sd* shell indicated. The closure of the $1p_{\frac{1}{2}}$ with N=8 provides a natural reference from which to examine the impact made by the presence of a few nucleons in the *sd* shell. Addition of two neutrons to ^{16}O, ^{17}F, and ^{18}Ne increases the interaction cross-section by 50, 61, and 68 mb respectively. Addition of two protons to ^{16}O, i.e. ^{18}Ne, results in an increase of σ_I by 94 mb while in the case ^{18}O to ^{20}Ne, it increases by 112 mb. The difference in the interaction cross-section with the addition of two protons (94-112 mb) as compared to addition of two neutrons (50-68 mb) is presumably due to the repulsion of the two protons with the ^{16}O core. Such a difference is not captured by systematics which relate the radius of a nucleus to simply the mass number, A, suggesting the advantage of using σ_I to account for trivial size effects.

*E-mail: deSouza@indiana.edu
[1]Corresponding author

Table 1: Interaction cross-sections for oxygen, fluorine, and neon nuclei with a carbon target at an energy about 900 A MeV. Taken from [10].

$^{18}Ne^{2p0n}$ σ_I=1076±25 mb	$^{20}Ne^{2p2n}$ σ_I=1144±10 mb
$^{17}F^{1p0n}$ σ_I=982±32 mb	$^{19}F^{1p2n}$ σ_I=1043±24 mb
$^{16}O^{0p0n}$ σ_I=982±6 mb	$^{18}O^{0p2n}$ σ_I=1032±26 mb

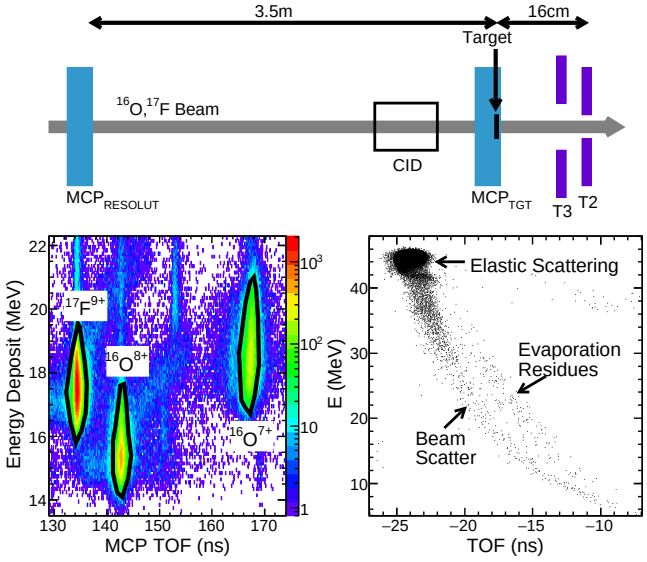


Figure 1: Schematic of the experimental setup along with a PID and ETOF spectra. Particle identification of the ^{17}F and ^{16}O ions incident on the target is displayed in the left plot along with a representative ETOF spectrum (selected on ^{17}F) used to identify evaporation residues (ER) in the right plot.

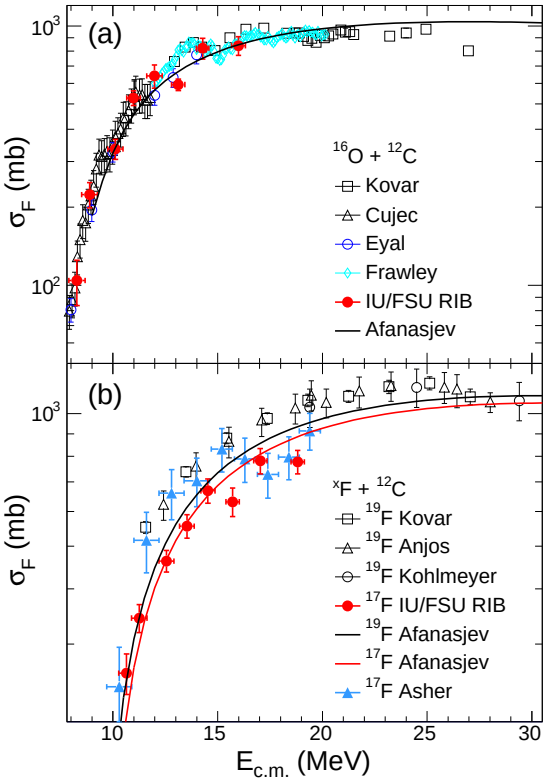


Figure 2: Fusion excitation functions for ^{16}O + ^{12}C (top panel) and ^{17,19}F + ^{12}C (bottom panel). The predictions of an analytic fusion model [12] are indicated by the solid lines.

While the excitation function for fusion of ^{16,18}O, ^{19}F, and ^{20}Ne ions with a carbon target already exists, no data exists for ^{17}F+^{12}C or ^{18}Ne+^{12}C. A beam of ^{16}O ions at Florida State University was used to produce ^{17}F ions via a (d,n) reaction. These ions were separated from the incident beam by the electromagnetic spectrometer RESOLUT [11]. The beam exiting the spectrometer consisted of both ^{17}F and residual ^{16}O ions necessitating identification of each ion on a particle-by-particle basis. The presence of both species allowed the simultaneous measurement of ^{16}O + ^{12}C and ^{17}F + ^{12}C providing a built-in reference measurement and comparison with the well-established fusion excitation function for ^{16}O + ^{12}C.

The setup used to measure fusion of fluorine and oxygen ions with carbon nuclei in this experiment is depicted in Fig. 1. Two microchannel plate detectors designated MCP$_{\rm RESOLUT}$ and MCP$_{\rm TGT}$ spaced ~3.5 m apart and a compact ionization detector (CID) permitted a ΔE-TOF measurement for each ion incident on the target. Measurement of the ΔE-TOF (Fig. 1) clearly shows three peaks corresponding to $^{17}F^{9+}$, $^{16}O^{7+}$, and $^{16}O^{8+}$ ions. The intensity of the ^{17}F beam incident on the target was 3-7 x 10^3 ions/s with a purity of 37%-54%.

Fusion of a ^{17}F (^{16}O) nucleus in the beam together with a ^{12}C nucleus in the target foil results in the production of an excited ^{29}P (^{28}Si) nucleus. For near-barrier collisions the excitation of the fusion product is relatively modest, E* ≈ 30 MeV. Emission of particles as the fusion product de-excites, deflects the evaporation residue (ER) from the beam direction. This deflection allows its detection and identification using two annular silicon detectors designated T2 and T3 that subtend the angular range $3.5° < \theta_{lab} < 25°$. Using the measured energy deposit in the silicon detectors and the time-of-flight [13], the mass of the ion was calculated. ERs were cleanly distinguished from beam particles by their mass[14, 15]. A representative ETOF spectrum is presented in Fig. 1.

The fusion cross-section, σ_F is extracted from the measured yield of evaporation residues through the relation σ_F = N$_{ER}$/(ϵ_{ER} x t x N$_I$) where N$_I$ is the number of beam particles of a given type incident on the target, t is the target thickness, ϵ_{ER} is the detection efficiency, and N$_{ER}$ is the number of evaporation residues detected. The number N$_I$ is determined by counting the particles with the appropriate time-of-flight between the two microchannel plates that additionally have the correct identification in the ΔE-TOF map depicted in Fig. 1. The target thickness, t, is 105 ± 0.5 μg/cm^2. The number of detected residues, N$_{ER}$, is determined by summing the number of detected residues clearly identified by the ETOF technique as shown in Fig. 1 [15]. To obtain the detection efficiency, ϵ_{ER}, a statistical model is used to describe the de-excitation of the fusion product together with the geometric acceptance of the experimental setup. The detection efficiency varied from ~81% at the highest incident energies measured to ~85% at the lowest

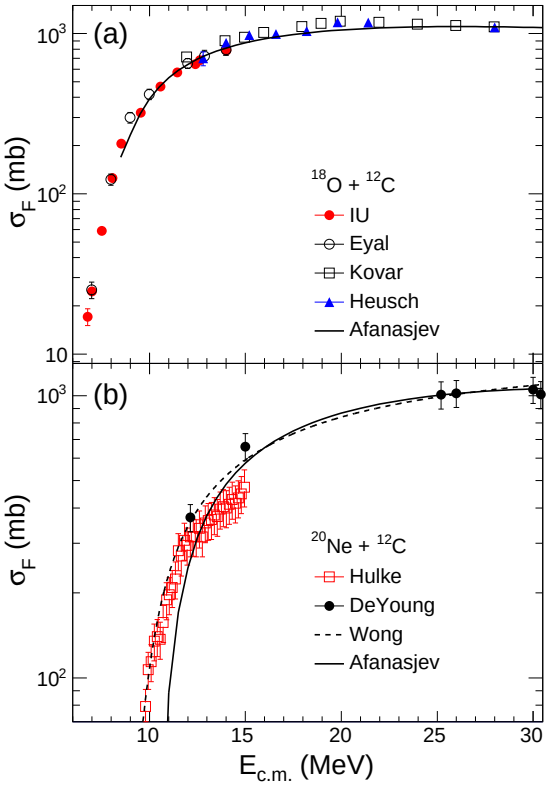


Figure 3: Fusion excitation functions for ^{18}O+^{12}C (top panel) and ^{20}Ne+^{12}C (bottom panel) together with the predictions of the analytic model[12]. The fit of the ^{20}Ne data by a one-dimensional barrier-penetration model [16] is depicted by the dashed line.

incident energy due to the changing kinematics of the reaction with an associated uncertainty of approximately 5%.

3. Results and Discussion

Depicted in Fig. 2 are the measured excitation functions for fusion of ^{16}O and ^{17}F ions with a carbon target. With the experimental technique used, both the ^{16}O + ^{12}C and ^{17}F + ^{12}C excitation functions are simultaneously measured. In the top panel, for ^{16}O, one observes the good agreement of this measurement, depicted as the solid (red) circles, with the experimental cross-sections reported in the literature [17, 18, 19, 20]. The present measurement reproduces the known resonances in the interval 10 MeV $\leq$E$_{c.m.}\leq$ 18 MeV demonstrating that the measurement of the fusion excitation function for ^{17}F + ^{12}C is robust. In the lower panel of Fig. 2 the measured cross-sections for ^{17}F+^{12}C (solid red circles) are presented along with the excitation function for ^{19}F+^{12}C. The multiple measurements for ^{19}F [21, 19, 22] are in agreement within the measurement uncertainties. As might be expected naively by the reduction of two neutrons, the ^{17}F-induced fusion of this measurement exhibits a lower cross-section than ^{19}F for all energies shown. The measured excitation functions are compared with the predictions of an analytic model based on a parameterization of the Sao Paulo potential model coupled with a barrier penetration formalism [12, 23, 24]. This model which has parameterized a large number of reactions for low and mid-mass systems is a useful tool for network simulations in the near-barrier regime. Despite having several fitted parameters, the analytic model has no adjustable parameters and thus serves as a useful benchmark of the expected systematic behavior. The above-barrier cross-sections predicted by this model are depicted in Fig. 2 as the solid lines. In the case of the ^{16}O fusion the analytic model provides a reasonable description of the overall behavior of the excitation function. The failure of the analytic model to reproduce the resonance is unsurprising as it assumes a smooth, structureless barrier. For the fluorine isotopes, while the excitation function for ^{17}F is reasonably described, the excitation function for ^{19}F is clearly underpredicted in the energy range measured. Nonetheless, the analytic model does predict an increase in the cross-section associated with the presence of the two additional neutrons in ^{19}F as compared to ^{17}F.

Also presented in Fig. 2 is the excitation function for ^{17}F + ^{12}C recently measured by Asher et al. (solid blue triangles) [25]. The statistical uncertainties of the Asher measurement are significantly larger than those of the present measurement. As importantly, the Asher measurement has significantly larger uncertainty in the energy, an inherent consequence of the technique utilized. Even considering the uncertainties of both excitation functions it is clear that the Asher excitation function reports larger cross-sections or is shifted to lower energies as compared to the present measurement. Surprisingly, the excitation function measured by Asher for E$_{c.m.}\leq$15 MeV is essentially consistent with the excitation function for ^{19}F. This result would imply that the removal of two neutrons from ^{19}F makes a negligible difference in both the barrier and the size of the fusing system. Such a result is inconsistent with the analytic model results which describes the expected systematic behavior. Consequently, for the remainder of this work only the present ^{17}F data is considered.

The excitation functions for fusion of ^{18}O and ^{20}Ne nuclei with carbon are shown in Fig. 3. While good agreement is observed for the various ^{18}O datasets, in the case of ^{20}Ne, for 12 MeV $\leq$E$_{c.m.}\leq$15 MeV a discrepancy exists between the measurements of Hulke [26] and deYoung [27]. This discrepancy at E$_{c.m.}$ ~15 MeV is larger than the reported uncertainties by both experimental measurements. Moreover, the shape of the excitation function determined by Hulke [26] deviates from the behavior of a smooth barrier as indicated by the analytic model [12]. The Hulke data [26] for E$_{c.m.}\leq$11 MeV and the deYoung data [27] can be described by a one-dimensional barrier penetration model [16] as indicated by the dashed line in Fig. 3.

In order to appropriately compare all the fusion excitation functions for these light nuclei, we scale the fusion cross-section by the interaction cross-section, σ_I, presented in Table 1. In addition, the trivial effect of the different barriers is accounted for by examining the reduced cross-section, σ_F/σ_I, as a function of the above-barrier energy, E$_{c.m.}$-V$_B$. The value of the barrier, V$_B$, is taken from the Bass model [28]. The uncertainties shown in the reduced cross-section reflect the uncertainties in both σ_F and σ_I. This presentation allows one to investigate differences between the nuclei shown after effectively eliminating systematic differences in the static size and barrier. Compar-

ison of all the excitation functions in Fig. 4 yields some interesting results. In Fig. 4a one observes that for ($E_{c.m.}$-V_B)≤9 MeV, the reduced cross-sections for ^{16}O and ^{18}O are relatively comparable. The prominent resonance structure for ^{16}O-induced fusion is absent in the case of ^{18}O. Above 9 MeV one observes that the reduced cross-section for ^{18}O exceeds that of ^{16}O. This increase in the reduced cross-section indicates the impact of the two *sd* neutrons on the fusion cross-section *over and above the increase in the static size*. In further understanding the role of *sd* valence nucleons on fusion, we elect to choose ^{18}O as our reference. The absence of strong, sharp resonance structures in the ^{18}O reaction supports this choice. To facilitate the use of ^{18}O as a reference we have described the data by the smooth curve depicted in Fig. 4a. This curve corresponds to a third-order polynomial fit to the reduced cross-sections for ^{18}O and simply serves as an adequate representation of the ^{18}O data in Fig. 4b.

Presented in Fig. 4b are the reduced excitation functions for ^{19}F, ^{20}Ne, and ^{17}F in comparison to ^{18}O. Within the measurement uncertainties the ^{19}F data manifests the same reduced cross-section as the ^{18}O. However, there is a subtle indication that the reduced cross-section for ^{19}F appears to be systematically slightly lower than that of ^{18}O for ($E_{c.m.}$-V_B)≥9 MeV. The $\langle\sigma_F/\sigma_I\rangle$ in this energy interval is 1.11±0.04 for ^{18}O and 1.06±0.07 for ^{19}F. This comparison between ^{18}O and ^{19}F is complicated by the presence of the unpaired proton in ^{19}F.

Examination of the reduced cross-section for ^{20}Ne is more telling. For all energies measured, the ^{20}Ne reduced cross-section is lower than that of both ^{18}O and ^{19}F. Unfortunately, lack of data between ~5 MeV≤($E_{c.m.}$-V_B)<15 MeV prevents a better characterization of this excitation function. The reduced cross-sections for ^{17}F observed in this work are reduced as compared to the cross-sections for ^{19}F for the entire energy range measured. This decreased value for ^{17}F as compared to ^{19}F is qualitatively consistent with the trend observed for ^{18}O and ^{16}O.

To investigate the interaction of the valence protons on the valence neutrons we have performed Relativistic Mean Field (RMF) calculations of the neutron and proton density distributions of light nuclei. In examining the proton and neutron density distributions for neutron-rich carbon nuclei from these RMF calculations, one observes that with increasing neutron number not only does the tail of the neutron density distribution extend further out but despite a constant number of protons, the proton density distribution is slightly extended [29]. This interaction between valence protons and neutrons is also reflected in the one proton separation energies of ^{16}O,^{18}O,and ^{20}O which are 12.1, 15.9, and 19.3 MeV respectively.

Based upon these calculations we hypothesize that the slight decrease in the cross-section for ^{19}F as compared to ^{18}O could reflect the attraction of the *sd* proton on the two *sd* neutrons resulting in a reduction of the fusion probability. The lower cross-sections for ^{20}Ne as compared to ^{18}O and ^{19}F is similarly consistent with the attraction of the two *sd* protons on the two *sd* neutrons and the consequent suppression of fusion. It should be appreciated that the explanation of these observations is at a qualitative level and a more quantitative description will require more sophisticated theoretical calculations which include

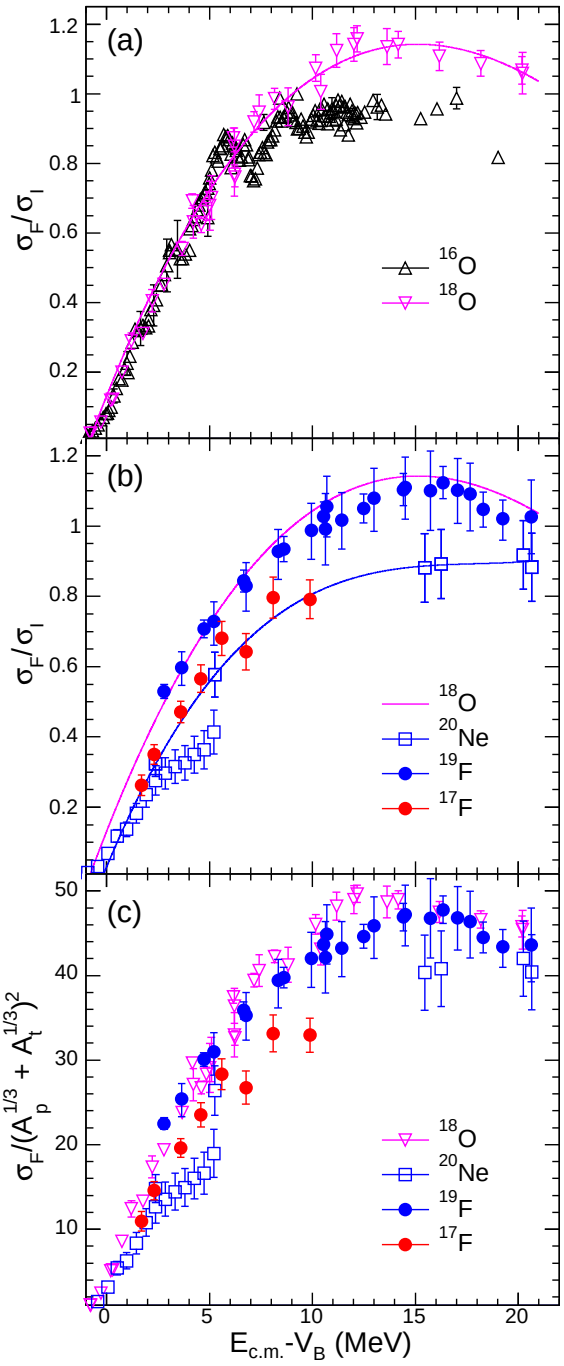


Figure 4: Comparison of the reduced excitation functions for fusion of ^{16}O and ^{18}O ions (top panel) and ^{18}O, ^{20}Ne, ^{19}F, and ^{17}F ions (lower panels) on a carbon target. The line through the ^{20}Ne data simply serves to guide the eye.

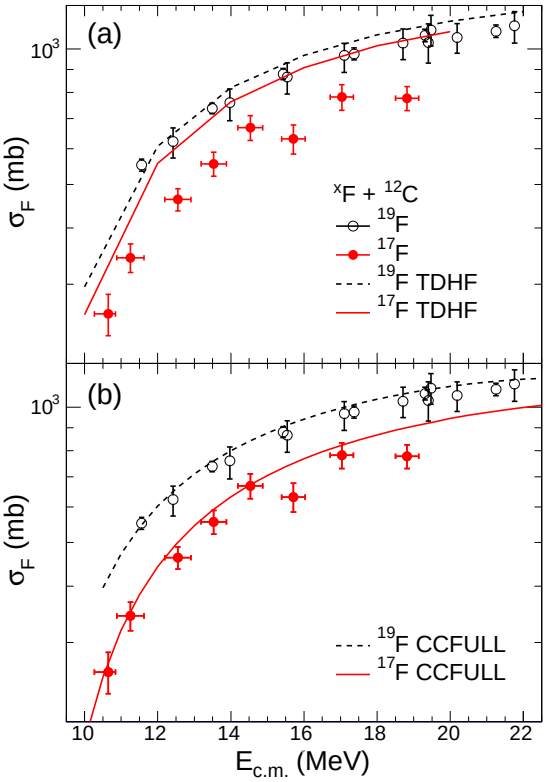


Figure 5: Comparison of the fusion excitation function for ^{17,19}F+^{12}C with the predictions of a TDHF model (panel a) and CCFULL (panel b).

nuclear structure.

These observations for the fusion of light *sd* nuclei can be summarized as follows. The fusion cross-section is enhanced by the presence of *sd* neutrons. This increased cross-section is suppressed by the presence of *sd* protons. It should be stressed that these changes in the reduced fusion cross-section relative to the barrier are beyond the systematic changes expected. It is clear that further experimental data, particularly in the case of ^{20}Ne and ^{17}F would be extremely useful. To assess the sensitivity of our results to the use of the interaction cross-section, σ_I, as a reference, we have calculated the reduced cross-section as $\sigma_F/(A_P^{\frac{1}{3}}+A_T^{\frac{1}{3}})^2$ where A_P and A_T are the mass number of the projectile and target nuclei respectively. While more sophisticated prescriptions for the reduced cross-section have been utilized in comparing dissimilar systems, given the similarity of the systems compared in this work this simple scaling is appropriate [30]. Examining the dependence of this quantity on ($E_{c.m.}$-V_B) in Fig. 4c reveals that although the reduced cross-section for ^{20}Ne lies closer to that of ^{19}F, the trends observed in Fig. 4b remain the same indicating the robustness of the observations.

To investigate the role of dynamics in the ^{17,19}F + ^{12}C reaction we performed time-dependent Hartree Fock calculations. On general grounds the TDHF approach is well-suited to describing the large-amplitude collective motion associated with fusion. Artificial symmetry restrictions are eliminated by performing the TDHF calculations on a 3D cartesian grid [31]. Recent calculations [32] have provided a good description of above-barrier fusion data [33, 34]. The TDHF calculations were performed by initiating collisions for increasing impact parameters in steps of 0.01 fm until the maximum impact parameter for fusion is reached. Calculations were performed using the Sky3D model [35], with a SV-bas interaction with DDDI pairing. It should be noted that pairing significantly impacts the fusion cross-section in TDHF [15] emphasizing the need for its accurate description. The results of the TDHF calculations for ^{17}F and ^{19}F are depicted in Fig. 5a as the solid and dashed lines respectively. While the model provides a reasonable description of the ^{19}F data, the ^{17}F cross-sections are overpredicted. It should be noted that TDHF calculations often slightly overpredict the above-barrier cross-sections due to their neglect of breakup processes, complicating direct comparison of the cross-section. Nonetheless, it is noteworthy that the difference between ^{19}F and ^{17}F observed experimentally is not reproduced.

Coupled-channels calculations [36, 37] have been performed to assess the relative importance of the ground and excited states on the fusion cross-section. Results of CCFULL calculations [38] in which only the ground state of both target and projectile nuclei is considered are presented in Fig. 5b. A reasonable description of both excitation functions is achieved. Inclusion of excited states acts to increase the cross-section slightly, though primarily at sub-barrier energies. The limited impact of excited states on fusion of ^{17}F in this near-barrier regime is consistent with other measurements [25, 7]. This description of the measured cross-sections corresponds to a potential in CCFULL with R_B= 7.89 fm, V_B=9.17 MeV, and $\hbar\omega$=3.36 MeV for ^{17}F and R_B= 8.42 fm, V_B=8.58 MeV, and $\hbar\omega$=2.94 MeV for ^{19}F. While the limited span of the experimental data does not permit a reliable extraction of $\hbar\omega$, the trend of increasing R_B and decreasing V_B with the addition of two neutrons is qualitatively understandable reflecting the increased nuclear interaction.

4. Summary

Systematic comparison of the fusion excitation functions for isotopes of O, F, and Ne nuclei with a carbon target can be used to examine the impact of valence *sd* protons and neutrons on fusion. After accounting for differences in the static size of the incident nuclei and systematic changes in the fusion barrier, differences are noted between fusion of ^{18}O, ^{19}F, ^{17}F, and ^{20}Ne with a carbon target. At energies about 5 MeV above the barrier the reduced cross-section for ^{17}F decreases as compared to ^{19}F. This decrease is similar to the one observed for ^{16}O as compared to ^{18}O. The observed trend can be interpreted as the influence of *sd* protons and neutrons on the reduced cross-section. In this framework, at energies upto 20 MeV above the barrier the presence of valence *sd* neutrons acts to increase the effective size of the system that fuses *above the increase in the static size*. Both the ^{16}O/^{18}O and ^{17}F/^{19}F manifest this behavior. Comparison of a nucleus with *sd* protons and neutrons to one with *sd* neutrons alone indicates that the presence of the *sd* protons results in a decrease of the effective size. This behavior is interpreted as the strong interaction between the *sd* protons

and the *sd* neutrons. It should be emphasized that this explanation of the trends noted is qualitative and a quantitative description which requires an accurate description of pairing effects is not yet available. Both a widely-used analytic model of fusion and a state-of-the-art dynamical model were used to investigate the systematic behavior expected. While both models predict a decrease in the cross-section with removal of *sd* neutrons, the magnitude of the observed reduction in the fusion cross-section for ^{17}F as compared to ^{19}F is not reproduced. Coupled-channels calculations which consider only the ground state nuclei are able to reproduce the measured excitation functions despite the presence of the low-lying $2s_{1/2}$ proton-halo state. This initial observation of the sensitive interplay of valence neutrons and protons in the fusion of *sd* shell nuclei motivates further high-quality measurements of fusion for neutron-rich light nuclei. A new generation of radioactive beam facilities [3, 2], and in particular the availability of low-energy reaccelerated beams, provides an unprecedented opportunity to explore this topic and improve our understanding of low-density nuclear matter.

5. Acknowledgements

This work was supported by the U.S. Department of Energy under Grant Nos. DE-FG02-88ER-40404 (Indiana University), and the National Science Foundation under Grant No PHY-1491574 (Florida State University). J.V. acknowledges the support of a NSF Graduate Research Fellowship under Grant No. 1342962.

References

[1] B. Back, H. Esbensen, C. Jiang, K. Rehm, Recent developments in heavy-ion fusion reactions, Rev. Mod. Phys. 86 (2014) 317–360.

[2] GANIL, Grand Accelérateur National d'Ions Lourds, Caen, France. [link].
URL http://www.ganil-spiral2.eu/

[3] FRIB, Facility for Rare Isotope Beams, Michigan State University, USA. [link].
URL http://frib.msu.edu

[4] A. S. Umar, V. E. Oberacker, C. J. Horowitz, Microscopic sub-barrier fusion calculations for the neutron star crust, Phys. Rev. C 85 (2012) 055801. doi:10.1103/PhysRevC.85.055801.

[5] R. Morlock, R. Kunz, A. Mayer, M. Jaeger, A. Müller, J. W. Hammer, P. Mohr, H. Oberhummer, G. Staudt, V. Kölle, Halo properties of the first 1/2+ state in ^{17}f from the ^{16}O(p,γ)^{17}F reaction, Phys. Rev. Lett. 79 (1997) 3837. doi:10.1103/PhysRevLett.79.3837.

[6] J. Kolata, V. Guimaraes, E. Aguilera, Elastic scattering, fusion, and breakup of light exotic nuclei, Eur. Phys. J. A 52 (2016) 123. doi:10.1140/epja/i2016-16123-1.

[7] K. E. Rehm, H. Esbensen, C. L. Jiang, B. B. Back, F. Borasi, B. Harss, R. V. F. Janssens, V. Nanal, J. Nolen, R. C. Pardo, M. Paul, P. Reiter, R. E. Segel, A. Sonzogni, J. Uusitalo, A. H. Wuosmaa, Fusion cross sections for the proton drip line nucleus ^{17}f at energies below the coulomb barrier, Phys. Rev. Lett. 81 (1998) 3341. doi:10.1103/PhysRevLett.81.3341.

[8] I. Tanihata, et al., Measurements of interaction cross sections and radii of He isotopes, Phys. Lett. B 160 (1985) 380–384. doi:10.1016/0370-2693(85)90005-X.

[9] I. Tanihata, et al., Measurements of Interaction Cross Sections and Nuclear Radii in the Light p-Shell Region, Phys. Rev. Lett. 55 (1985) 2676–2679. doi:10.1103/physrevlett.55.2676.

[10] A. Ozawa, T. Suzuki, I. Tanihata, Nuclear size and related topics, Nucl. Phys. A 693 (2001) 32.

[11] I. Wiedenhöver, et al., Studies of exotic nuclei at the RESOLUT facility at Florida State University, in: J. Hamilton, A. Ramayya (Eds.), Fifth International Conference on Fission and Properties of Neutron-rich Nuclei, World Scientific, 2012, p. 144.

[12] A. Afanasjev, M. Beard, A. I. Chugunov, M. Wiescher, D. Yakolev, Large collection of astrophysical s factors and their compact representations, Phys. Rev. C 85 (2012) 054615. doi:10.1103/PhysRevC.85.054615.

[13] R. T. deSouza, et al., Sub-nanosecond time-of-flight for segmented silicon detectors, Nucl. Instr. Meth. A 632 (2011) 133. doi:10.1016/j.nima.2010.12.101.

[14] T. K. Steinbach, et al., Measuring the fusion cross-section of light nuclei with low-intensity beams, Nucl. Instr. Meth. A 743 (2014) 5. doi:10.1016/j.nima.2013.12.045.

[15] T. K. Steinbach, J. Vadas, J. Schmidt, C. Haycraft, S. Hudan, R. T. deSouza, L. T. Baby, S. A. Kuvin, I. Wiedenhöver, A. S. Umar, V. E. Oberacker, Sub-barrier enhancement of fusion as compared to a microscopic method in ^{18}O + ^{12}C, Phys. Rev. C 90 (2014) 041603(R). doi:10.1103/PhysRevC.90.041603.

[16] W. C.Y., Interaction barrier in charged-particle nuclear reactions, Phys. Rev. Lett. 31 (1973) 766–769. doi:10.1103/PhysRevLett.31.766.

[17] B. Cujec, C. Barnes, Total reaction cross section for ^{12}C + ^{16}O below the Coulomb barrier, Nucl. Phys. A 266 (1976) 461–493.

[18] Y. Eyal, M. Beckerman, R. Chechik, Z. Fraenkel, H. Stocker, Nuclear size and boundary effects on fusion barrier of oxygen with carbon, Phys. Rev. C 13 (1976) 1527–1535. doi:10.1103/PhysRevC.13.1527.

[19] D. G. Kovar, et al., Systematics of carbon- and oxygen-induced fusion on nuclei with 12 $\leq$A$\leq$ 19, Phys. Rev. C 20 (1979) 1305–1331. doi:10.1103/PhysRevC.20.1305.

[20] A. D. Frawley, N. R. Fletcher, L. C. Dennis, Resonances in the ^{16}O + ^{12}C fusion cross section between $E_{\mathrm{c.m.}}$ = 12and20 mev, Phys. Rev. C 25 (1982) 860–865. doi:10.1103/PhysRevC.25.860.

[21] B. Kohlmeyer, W. Pfeffer, F. Puhlhofer, Fusion and direct reactions between 92 MeV ^{19}F and ^{12}C, Nucl. Phys. A 292 (1977) 288–300.

[22] R. Anjos, et al., Effect of the entrance channel mass asymmetry on the limitation of light heavy-ion fusion cross sections, Phys. Rev. C 42 (1990) 354. doi:doi.org/10.1103/PhysRevC.42.354.

[23] M. Beard, A. Afanasjev, L. Chamon, L. Gasques, Astrophysical s-factors for fusion reactions involving C,O, Ne and Mg isotopes, Atomic Data and Nuclear Data Tables 96. doi:10.1016/j.adt.2010.02.005.

[24] D. Yakolev, M. Beard, L. Gasques, M. Wiescher, Simple analytic model for astrophysical S factors, Phys. Rev. C 82 (2010) 044609. doi:10.1103/PhysRevC.82.044609.

[25] B. W. Asher, S. Almaraz-Calderon, V. Tripathi, K. W. Kemper, L. T. Baby, N. Gerken, E. Lopez-Saavedra, A. B. Morelock, J. F. Perello, I. Wiedenhover, Experimental study of the ^{17}f+ ^{12}c fusion reaction and its implications for fusion of proton-halo systemsArXiv:2010.05819.

[26] G. Hulke, C. Rolfs, H. Trautvetter, Comparison of Fusion Reactions ^{12}C + ^{20}Ne and ^{16}O + ^{16}O near the Coulomb Barrier, Z. Physik A 297 (1980) 161.

[27] P. deYoung, J. J. Kolata, R. Luhn, R. Malmin, S. Tripathi, Gamma-ray studies of ^{12}C + ^{20}Ne reactions, Phys. Rev. C 25 (1982) 1420.

[28] R. Bass, Nuclear Reactions with Heavy Ions, Springer Verlag, 1980.

[29] R. deSouza, V. Singh, S. Hudan, Z. Lin, C. Horowitz, Extracting dynamics in the fusion of neutron-rich light nucleiArXiv:2007.11406.

[30] L. Canto, D. M. Junior, P. Gomes, J. Lubian, Reduction of fusion and reaction cross sections at near-barrier energies, Phys. Rev C 92 (2015) 014626. doi:10.1103/PhysRevC.92.014626.

[31] A. S. Umar, V. E. Oberacker, Three-dimensional unrestricted time-dependent Hartree-Fock fusion calculations using the full Skyrme interaction, Phys. Rev. C 73 (2006) 054607. doi:10.1103/PhysRevC.73.054607.

[32] K.-H. Kim, T. Otsuka, P. Bonche, Three-dimensional TDHF calculations for reactions of unstable nuclei, Journal of Physics G: Nuclear and Particle Physics 23 (10) (1997) 1267–1273. doi:10.1088/0954-3899/23/10/014.

[33] C. Simenel, B. Avez, Time-dependent hartree-fock description of heavy ions fusion, Int. Jou. of Mod. Phys. E 17 (2008) 31–40. doi:10.1142/S0218301308009525.

[34] C. Simenel, A. Umar, K. Godbey, M. Dasgupta, D. Hinde, How the pauli exclusion principle affects fusion of atomic nuclei, Phys. Rev. C 95 (2017) 031601. doi:10.1103/PhysRevC.95.031601.

[35] B. Schuetrumpf, P.-G. Reinhard, P. D. Stevenson, A. S. Umar, J. A. Maruhn, The TDHF code Sky3d version 1.1, Computer Physics Communications 229 (2018) 211–213. doi:10.1016/j.cpc.2018.03.012.

[36] C. Dasso, S. Landowne, A. Winther, Channel-coupling effects in heavy-ion fusion reactions, Nucl. Phys. A 405 (1983) 381–396. doi:10.1016/0375-9474(83)90578-x.

[37] H. Esbensen, Coupled-channels calculations for ^{16}O + ^{16}O fusion, Phys. Rev C 77 (2008) 054608. doi:10.1103/PhysRevC.77.054608.

[38] K. Hagino, N. Rowley, A. T. Kruppa, A program for coupled-channel calculations with all order couplings for heavy-ion fusion reactions, Comput. Phys. Commun. 123 (1999) 143–152. doi:10.1016/s0010-4655(99)00243-x.